

A SPECTROSCOPIC CONFIRMATION OF THE BOÖTES II DWARF SPHEROIDAL¹

ANDREAS KOCH², MARK I. WILKINSON³, JAN T. KLEYNA⁴, MIKE IRWIN⁵, DANIEL B. ZUCKER⁵,
VASILY BELOKUROV⁵, GERARD F. GILMORE⁵, MICHAEL FELLHAUER^{5,6}, AND N. WYN EVANS⁵

Accepted for publication in the Astrophysical Journal

ABSTRACT

We present a new suite of photometric and spectroscopic data for the faint Boötes II dwarf spheroidal galaxy candidate. Our deep photometry, obtained with the INT/WFC, suggests a distance of 46 kpc and a small half-light radius of 4.0' (56 pc), consistent with previous estimates. Follow-up spectroscopy obtained with the Gemini/GMOS instrument yielded radial velocities and metallicities. While the majority of our targets covers a broad range in velocities and metallicities, we find five stars which share very similar velocities and metallicities and which are all compatible with the colors and magnitudes of the galaxy's likely red giant branch. We interpret these as a spectroscopic detection of the Boötes II system. These stars have a mean velocity of -117 km s^{-1} , a velocity dispersion of $(10.5 \pm 7.4) \text{ km s}^{-1}$ and a mean $[\text{Fe}/\text{H}]$ of -1.79 dex, with a dispersion of 0.14 dex. At this metallicity, Boo II is not consistent with the stellar-mass-metallicity relation for the more luminous dwarf galaxies. Coupled with our distance estimate, its high negative systemic velocity rules out any physical connection with its projected neighbor, the Boötes I dwarf spheroidal, which has a velocity of $\sim +100 \text{ km s}^{-1}$. The velocity and distance of Boötes II coincide with those of the leading arm of Sagittarius, which passes through this region of the sky, so that it is possible that Boötes II may be a stellar system associated with the Sagittarius stream. Finally, we note that the properties of Boötes II are consistent with being the surviving remnant of a previously larger and more luminous dSph galaxy.

Subject headings: galaxies: dwarf — galaxies: individual (Boötes I, Boötes II, Sagittarius) — galaxies: kinematics and dynamics — galaxies: stellar content

1. INTRODUCTION

Dwarf spheroidal galaxies (dSphs) are a well-established mainstay in discussions of cosmological structure formation. Although these small-scale systems are clearly dark matter dominated (Mateo 1998; Gilmore et al. 2007), the properties of the more luminous dSphs are difficult to reconcile with a simplistic building block scenario (e.g., Unavane et al. 1996; Moore et al. 1999; Venn et al. 2004). In this context, proposed solutions to major controversies such as the missing satellite problem (Robertson et al. 2005; Font et al. 2006; Strigari et al. 2007; Simon & Geha 2007; Bovill & Ricotti 2008) have been further fueled by a plethora of discoveries of even fainter dSph candidates around the Milky Way using data from the Sloan Digital Sky Survey (SDSS; Willman et al. 2005a,b; Zucker et al. 2006; Belokurov et al. 2006a, 2007; Walsh et al. 2007a). Characteristic properties of these systems are very low luminosities and low stellar masses, while the apparently high mass-to-light ratios (of up to several hundreds) seen in several of them

(Simon & Geha 2007) are usually taken as indicative of a dominant dark matter component.

Gilmore et al. (2007) showed that there is a minimum half-light radius of $\sim 100 \text{ pc}$ for all isolated dSphs more than 50 kpc from the Galactic centre, and a maximum half-light radius of equilibrium (dark matter-free) globular clusters (GCs) of $\sim 30 \text{ pc}$. They suggested this minimum size is an intrinsic feature of systems with dark matter halos. For this to be true, the few very-low luminosity objects in or close-to the corresponding size gap would be tidally disrupting/disrupted dSphs or star clusters. The radius distribution has been confirmed in a subsequent analysis of SDSS photometric data (Martin et al. 2008). The characterisation of the few observed systems of sizes intermediate between dSphs and star clusters is thus a test of the minimum size relation proposed by Gilmore et al. (2007). To show that such a system is a former dSph would require detecting a residual or truncated dark matter halo and/or a large intrinsic chemical abundance dispersion.

Among the new ultra-faint objects is Boötes II (hereafter Boo II), which was identified as a stellar overdensity on the sky by Walsh et al. (2007a) and which exhibits a vague main sequence turnoff (MSTO) and only a sparse red giant branch (RGB). Boo II is among the four faintest dSph candidates presently known ($M_V = -2.7$; Martin et al. 2008). Moreover, its spatial extent ($\sim 36\text{--}50 \text{ pc}$; Walsh et al. 2007b; Martin et al. 2008) renders it incompatible with a classical GC which has been unaffected by tides. Its small projected separation (only 1.6°) from the faint Boötes I dSph and its radial distance of 42 kpc (Walsh et al. 2007b), close to that of Boötes I (ca. 60 kpc; Belokurov et al. 2006a; Siegel 2006; Dall'Ora et al.

Electronic address: akoch@astro.ucla.edu

¹ Based on observations made with the Isaac Newton Telescope operated on the island of La Palma by the Isaac Newton Group in the Spanish Observatorio del Roque de los Muchachos of the Instituto de Astrofísica de Canarias.

² UCLA, Department of Physics & Astronomy, 430 Portola Plaza, Los Angeles, CA 90095, USA

³ Dept. of Physics and Astronomy, University of Leicester, University Road, Leicester LE1 7RH, UK

⁴ Institute for Astronomy, Honolulu, 2680 Woodlawn Drive, Honolulu, HI 96822, USA

⁵ Institute of Astronomy, Madingley Road, Cambridge, CB3 0HA, UK

⁶ Departamento de Astronomía, Universidad de Concepción, Casila 160-C, Concepción, Chile

2006) prompted the suggestion that these two systems might be in some way associated. However, despite a mild degree of distortion in the isophotes of Boötes I, there is no current evidence of any interaction between these systems, which might be expected to give rise to aligned elongations in each dSph (see also Fellhauer et al. 2008). Although photometric studies suggest that Boo II is an old, metal-poor system (Walsh et al. 2007a,b), nothing is yet known about its kinematics.

In this work we investigate the physical nature of Boo II based on deep photometry and spectroscopic follow-up of this stellar system, by means of which we aim to measure its velocity and metallicity. In this way we can determine whether there is any possible connection between the pair of Boötes and constrain some of the important properties of Boo II. This Paper is organized as follows: in §2, the photometric and spectroscopic data and their reduction are described, while §3 focuses on the derivation of radial velocities and metallicities, based on which we claim a spectroscopic detection of Boo II. After a discussion of the possible nature of Boo II in §4 we summarize our findings in §5.

2. DATA AND REDUCTION

2.1. Photometry

Boo II was observed in sub-arcsec seeing conditions on the night of 2007 May 11 using the Wide Field Camera on the 2.5-m Isaac Newton Telescope (INT) on La Palma. The images were corrected for non-linearity, bias-corrected, trimmed, flat-fielded and defringed (i' only) using the processing pipeline developed by Irwin & Lewis (2001). This software was then used to generate detected object catalogues for each individual exposure (3×900 s for g' and 3×600 s for i'). The catalogues were used to refine the World Coordinate System information for each image prior to forming the deep image stacks and subsequently-generated deep catalogues that form the basis for the rest of this analysis. A preliminary photometric calibration was based on Landolt (1992) standard fields observed throughout the night. Since the night was partially non-photometric, due to varying levels of dust extinction, we then bootstrapped the data onto the SDSS photometric system using a table of SDSS stars from that region. In the SDSS AB system, the stacked data reach a 5σ depth of approximately 25.5 in g and 24.0 in i .

Figure 1 shows the resulting color-magnitude diagrams (CMDs) for the central five arcmin of Boo II (corresponding to about 1.2 half-light radii r_h ; e.g., Martin et al. 2008) and an offset control field located $15.6'$ ($3.7 r_h$) from the center of Boo II on an adjacent CCD (#2) detector. The right-hand panel of the figure shows the luminosity function (LF) in the central field together with a comparison LF derived from a larger area of CCD #2 and normalised to the same area as the central region. While there is a clear excess of stars in the main sequence and turn-off regions ($g-i \sim 0.25$, $21.5 < i < 24.0$), at brighter magnitudes where the sub-giant and RGB loci are expected, and from where we draw our spectroscopic targets, there is a much weaker excess.

2.2. Spectroscopy

We obtained spectra for seventeen stars in the field of Boo II using a single pointing of the GMOS-N spectro-

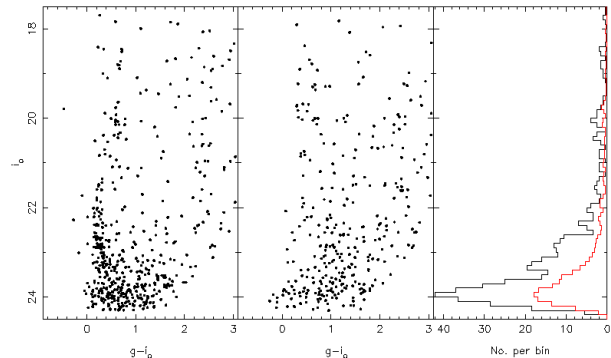


FIG. 1.— *Left panel:* $(g-i, i)$ CMD for stars within five arcmin of the center of Boo II. *Middle:* CMD for stars in a field offset by $15.6'$ from the centre of Boo II covering the same area as that of the central field. The right panel shows the i -band luminosity functions of stars in the central field (black) and from a much larger offset region (red line) suitably area-normalised. There is a clear excess of stars on the main sequence of Boo II and a smaller but still significant excess for turn-off and sub-giant stars.

graph, mounted on the Gemini North telescope, on 2007 April 17. Our targets were chosen by cross-matching of GMOS-N i -band pre-images with existing SDSS photometry. All target stars were selected to lie in the region of the CMD occupied by the sparse RGB of Boo II (see Figures 1,6). These are listed in Table 1 with their characteristic properties.

A single GMOS slit mask was prepared with slitlets of width $0.75''$. The spectra were centered on the spectral region containing the Ca II triplet (CaT) lines. Exposures were taken at central wavelengths of both 8550 and 8600Å in order to achieve continuous wavelength coverage in the spectra across the gaps between the CCDs. Our observations used the R831+_G5302 grating and CaT_G0309 filter, with 2×2 binning in the spectral and spatial dimensions. The spectra thus obtained have a nominal resolution of 3600. The total integration time was 12600s, which we divided into individual exposures of 1800s to facilitate cosmic ray removal.

The raw data were reduced using the standard *gemini* reduction package within the Image Reduction and Analysis Facility (IRAF). CuAr lamp exposures adjacent in time to the science exposures provided the calibration frames. The typical r.m.s. uncertainty in the wavelength calibration, obtained by fitting a polynomial to the line positions in the CuAr spectra, was 0.04\AA , which corresponds to a velocity uncertainty of $\sim 1.4 \text{ km s}^{-1}$ at the CaT. Typically, the final spectra have per-pixel signal-to-noise (S/N) ratios which range from very low quality (S/N as low as 3–5) up to ~ 25 , with a median S/N of 12. Three sample spectra of stars covering a representative magnitude range are shown in Fig. 2.

3. ANALYSIS

3.1. Structural parameters

TABLE 1
CHARACTERISTICS OF TARGET STARS. MAGNITUDES ARE THOSE FROM THE SDSS.

ID	α (J2000.0)	δ	i	g-i	v_{HC}^{V} [km s ⁻¹]	σ^{V}	[Fe/H]	σ [Fe/H]	S/N	Quality	Membership
1	13:58:07.2	12:51:47.5	19.04	0.41	-165.55	4.73	-1.53	0.12	17		
2	13:58:08.6	12:51:15.4	20.05	0.55	-131.49	8.48	-1.72	0.14	12		Boo II
3	13:58:09.5	12:51:25.5	19.83	0.67	-109.38	5.28	-1.74	0.12	14		Boo II
4	13:58:08.1	12:53:53.1	19.99	0.96	35.49	5.39	-0.84	0.18	10		
5	13:58:10.5	12:55:41.8	20.25	0.85	66.00	15.1	-0.80	0.22	8		
6	13:58:05.9	12:51:12.2	22.38	0.14	-88.86	15.0	3	s	
7	13:58:01.5	12:51:04.7	18.83	0.75	-125.58	4.07	-1.99	0.10	21		Boo II
8	13:58:00.7	12:53:45.0	19.14	0.52	95.93	3.17	-1.24	0.13	17		
9	13:57:59.8	12:54:26.1	18.52	0.84	-123.08	1.87	-1.61	0.11	28		Boo II
10	13:58:00.3	12:55:39.9	17.51	1.05	-4.44	1.76	-0.82	0.13	55		
11	13:58:02.6	12:51:35.9	21.42	0.49	-90.57	28.8	4	n	
12	13:58:01.9	12:53:45.9	22.00	0.82	238.11	6.25	3	s	
13	13:57:57.2	12:53:15.8	20.54	0.57	4.26	7.70	-1.45	0.39	7		
14	13:57:58.4	12:53:31.5	21.42	0.70	-125.05	9.86	-1.02	0.23	4	a	
15	13:57:51.2	12:51:36.6	18.50	0.76	-100.07	2.33	-1.81	0.10	27		Boo II
16	13:57:53.4	12:55:15.3	18.88	0.87	-10.50	2.24	-0.57	0.15	20		
17	13:57:52.2	12:52:47.1	22.13	0.88	301.14	9.13	3	n	

NOTE. — Quality flags are: (a) Ambiguous CCF peak; (n) No CCF peak discernible; (s) Spurious velocity due to sky residuals. Boo II member candidates are marked in the last column. See text for details.

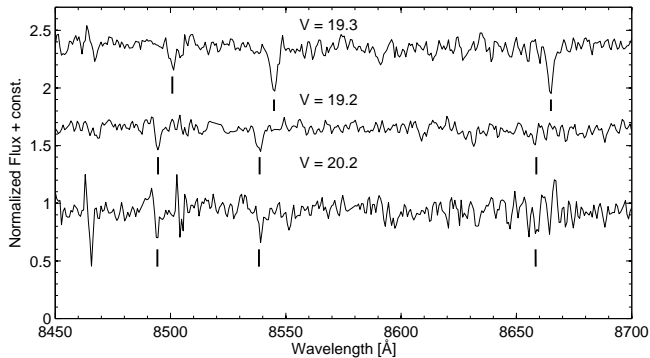


FIG. 2.— Sample spectra of a brighter foreground dwarf (top; S/N~17), and a typical (middle; SN~21) and fainter (bottom; SN~12) Boötes II giant candidate. The three CaT lines are indicated with vertical ticks. The Doppler shifts clearly separate the foreground star from the Boo II candidates.

Although two analyses of the structure of Boo II have been published already by Walsh et al. (2008) and Martin, de Jong & Rix (2008), the uncertainty in even the basic structural parameters is large enough to warrant further examination. Our relatively deep wide area photometry reaches well below the MSTO (see figure 1) and with a total coverage of 0.25 square degrees extends far enough from the main body of Boo II to enable a reliable background estimate. In particular, the published values for the half-light radius, r_h , central surface brightness, μ_0 , and absolute magnitude, M_v , emphasise the apparent hybrid nature of the object by locating it in the void between dwarf galaxies and stellar clusters (e.g. Belokurov et al. 2007).

To help further characterize the structure of Boo II we first constructed an isopleth (number density) map by counting stars satisfying $21.5 < g < 24.5$ and $g - i < 0.6$ on a 15 arcsec grid over a 0.5×0.5 degree region. We show in Fig. 3 a contour map of these number counts, smoothed with a Gaussian kernel of FWHM 1 arcmin. The “background” level, 0.60 ± 0.05 arcmin⁻², used here and for the subsequent profile analysis, was estimated from the average counts on CCD #2, the closest part of which is 11 arcmin to the West of the centre of Boo II.

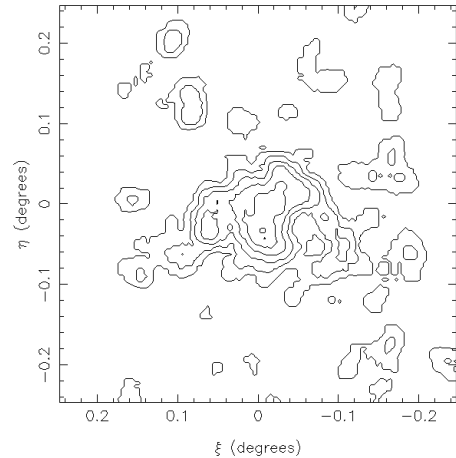


FIG. 3.— Contours of the number density of stellar objects satisfying $21.5 < g < 24.5$ and $g - i < 0.6$, N to the top and E to the left. These have been smoothed with a Gaussian of FWHM 1 arcmin and highlight the irregular appearance of Boo II. Contour levels begin at 0.5 arcmin⁻² above background, in steps of 0.5 arcmin⁻².

The highly irregular shape of Boo II renders an ellipticity and position angle estimate from our data difficult. Martin et al. (2008), from a maximum likelihood analysis, obtained values for ellipticity and position angle of 0.21 ± 0.21 and $-35^{\circ} \pm_{-55}^{+48}$, respectively, emphasising the uncertainty of imposing an elliptical morphology in a case like this.

We therefore decided to minimise the number of degrees of freedom and analyse the photometric properties of Boo II using circular annuli centred on our derived position of $(\alpha, \delta) = (13^{\text{h}}58^{\text{m}}05^{\text{s}}, 12^{\circ}52'0'')$. In this case the background-subtracted radial profile, from annuli spaced by 1 arcmin, is quite well-defined and is shown in figure 4 together with an overlaid model fit. A Plummer law with a central number density of 3.5 arcmin⁻² and half-light radius $r_h = 4.0^{+0.7}_{-0.3}$ adequately characterises the profile.

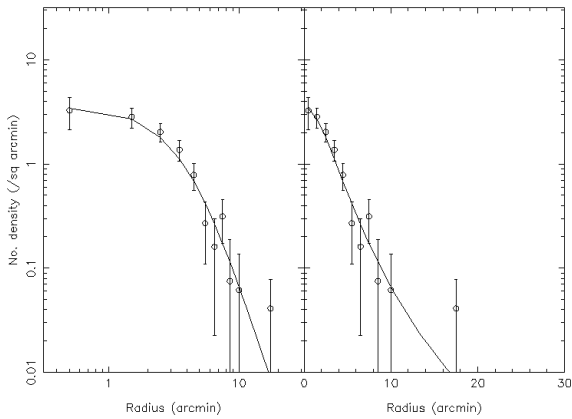


FIG. 4.— Background-corrected radial density profile of Boo II with the best-fit Plummer profile overlaid. The error bars include contributions from Poisson counting statistics and the error in the background estimate.

This value is in good agreement with the $4.2_{-1.4}^{+1.1}$ found by Martin et al. (2008), and somewhat larger than r_h of $2.5' \pm 0.5'$ from Walsh et al. (2007b). The profile in figure 4 is clearly not well-described by either a power law or an exponential, and, although a King model could no doubt be tailored to give an adequate fit, the extra degree of freedom and/or concept of a tidal radius for this system is hardly warranted.

The sparsity of potential Boo II CMD features brighter than the MSTO, its structural irregularity and the faintness of the system, make it difficult to derive an accurate direct estimate of the total magnitude. In contrast, however, the central surface brightness of the CMD region used in the profile analysis is quite well-defined. We therefore estimated what fraction of the total luminosity, and hence surface brightness, is contained in this region by comparison with the overall LF of M92 (Walsh et al. 2007a,b), assuming a similar stellar population for Boo II. Thus, by using only the well populated parts of the CMD (see Fig. 1) and re-scaling to correct for missing subgiants, RGB and fainter main sequence stars, we derive a central surface brightness in the Vega system of $\mu_{0,i} = 28.6$ and $\mu_{0,g} = 29.2$ mag arcsec $^{-2}$ with approximate error of ± 0.5 mag arcsec $^{-2}$. Integrating the Plummer profile then gives estimates of the total magnitude of $M_i \sim -2.7$ and $M_g \sim -2.1$. These are in good agreement with the values of $M_v = -2.7$ and $\mu_{0,v} = 28.5$ mag arcsec $^{-2}$ derived by Martin et al. (2008) and confirm the unusual position of Boo II in the r_h -versus- M_v ($\mu_{0,v}$) domain.

3.2. Radial velocities

Radial velocities of our targets were determined by cross correlation against a synthetic template, composed of the three CaT lines, using IRAF’s *fxcor* task. For the faintest stars, this procedure did not yield any clear correlation peak. We therefore followed Zucker (2003) in determining instead the cross correlation function (CCF) from each of the seven individual exposures of each star and subsequently combining the separate CCFs into a

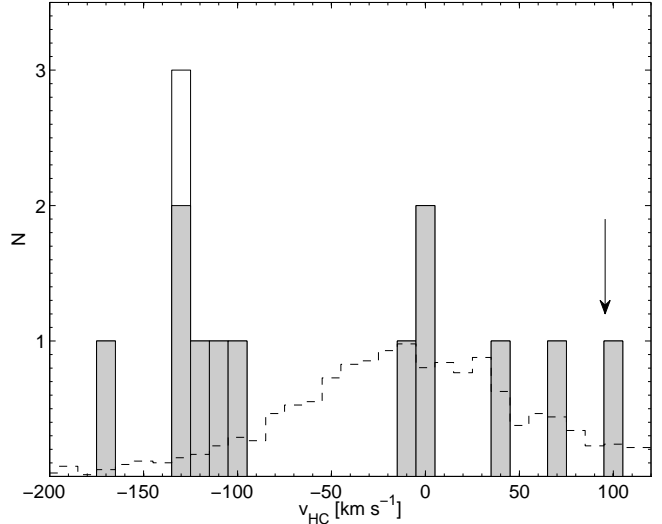


FIG. 5.— Velocity histogram of the 12 stars for which we could measure reliable velocities. The white bar indicates the target with only an ambiguous velocity signal in the CCF. The expected foreground contamination from the Galactic Besançon model (Robin et al. 2003) is shown as a dashed histogram. An arrow illustrates the systemic velocity of the Boötes I dSph.

straight average CCF for each target. This process efficiently increases our ability to detect the underlying velocity signal. In practice, the relative radial velocity was then determined from a Gaussian fit to the strongest average-CCF peak. The median radial velocity error on our measurements, as determined from the covariance matrix of the CCF fit (Zucker 2003), is 5.4 km s $^{-1}$.

The third CaT line at 8662\AA is prone to strong contamination by sky line residuals. While cross correlation against the third line only did not result in any measurable peaks in the CCF for most of the targets, its inclusion in the entire cross correlation region did not affect the derived velocities – the correlation of the entire CaT from $8475\text{--}8680\text{\AA}$ yields essentially the same velocities as a correlation restricted to only the first two lines at $\lambda\lambda 8498, 8542\text{\AA}$. For two of the faintest stars, no CCF was discernible at all and we discard these from further analysis (see the quality flag in Table 1). The low S/N spectra of the faint stars are particularly sensitive to sky removal and will inevitably contain stronger sky residuals compared to the weak absorption features. A cross correlation of a sky emission spectrum against the synthetic CaT template reveals that the strongest sky lines will produce spurious CCF peaks at -86 and $+240$ km s $^{-1}$, respectively (see also Kleyana et al. 2004). It is thus likely that the strong peaks at exactly these velocities in the CCFs of the two targets with i-band magnitudes of 22.0 and 22.4 mag (stars #6 and #12) are such sky residuals. We excluded these measurements from our sample as well. Finally, for one star the cross correlation yielded two peaks of comparable height, at ~ -120 and $+100$ km s $^{-1}$. We flagged this measurement as “dubious” (see Table 1) and continue by adopting the negative velocity, but account for its uncertain nature by both including and excluding it in the subsequent quantitative analyses. Our final set of heliocentric radial velocities, v_{HC} , is listed in Table 1 and shown in the histogram in Figure 5.

Those stars with velocities above -20 km s $^{-1}$ are certainly Galactic foreground stars as a comparison with

the Galactic Besançon model (Robin et al. 2003) confirmed (dashed line in Figure 5). While there is still a non-negligible fraction of Galactic contaminants expected below $\sim -100 \text{ km s}^{-1}$, we note the presence of an excess of stars at $\sim -120 \text{ km s}^{-1}$, which suggests a probable kinematic detection of Boo II member stars. If these were Galactic halo stars (as predicted by the model), it is curious that we do not see a more symmetric velocity distribution in our data; this again argues in favor of our having detected Boo II as an independent system. Moreover, a Kolmogorov-Smirnov test showed that the hypothesis that all stars with good velocities are from the same distribution as the Galactic model stars can be rejected at a 98% confidence level (2.3σ), while the sample *without* the Boo II candidates at -120 km s^{-1} is compatible with the foreground distribution at 35%, which again suggests that the stars in the negative velocity peak are likely not Galactic foreground.

3.3. Isochrone fits

In Figure 6 we show the location of our target stars in color-magnitude space. Stars belonging to the low-velocity peak are flagged as potential members (solid circles), while the likely foreground contaminants are shown as open symbols.

In order to obtain further insight into the possible association of each star with the Boo II overdensity, we compared the most prominent CMD features with a set of theoretical isochrones. For this purpose we performed a by-eye fit of a set of Solar-scaled isochrones from the Dartmouth group (Dotter et al. 2008) with a metallicity of -1.8 dex (see Sect. 3.3, 3.4) and a reddening of $E(B-V)=0.03$ (Schlegel et al. 1998), leaving age and distance modulus as free parameters. We note that the resulting “best-fit” isochrones are not sufficient to allow us to uniquely characterize the predominant stellar populations in Boo II or to derive an accurate distance modulus, but rather enable us to discuss the plausibility that our targets are Boo II members.

We find that the best fit using the isochrone corresponding to the spectroscopic metallicities ($[\text{Fe}/\text{H}] = -1.8$ dex) was preferred over more metal poor and more metal rich tracks, as also indicated by the globular cluster fiducials in Fig. 6. Neither of these simultaneously reproduce the MSTO and RGB. In particular, the MSTO of Boo II is bluer than the more metal poor GC M92 ($[\text{Fe}/\text{H}]=-2.4$), which may also suggest a slightly younger age for Boo II. Note that the best age, indicated by the isochrones, is 10–12 Gyr. In particular, a good fit is obtained for the RGB, TO and horizontal branch (HB) in the Hess diagram (bottom panel of Fig. 6), and also of the five individual suggested member stars (solid circles in Fig. 6, top panel). Moreover, the good fit of the (few) HB stars in the Boo II CMD assures us that the distance modulus could be estimated to within 0.2 mag accuracy. The resulting value of 18.3 mag (46 ± 4 kpc) is in good agreement with the measurement of 42 ± 2 kpc derived by Walsh et al. (2007b). All in all, our data appear to confirm Boo II as a moderately old and metal-poor population (Walsh et al. 2007a,b).

All stars with velocities in excess of -50 km s^{-1} are well separated from the isochrone in Fig. 6, with the exception of #13 (with $+4 \text{ km s}^{-1}$). The target at -165

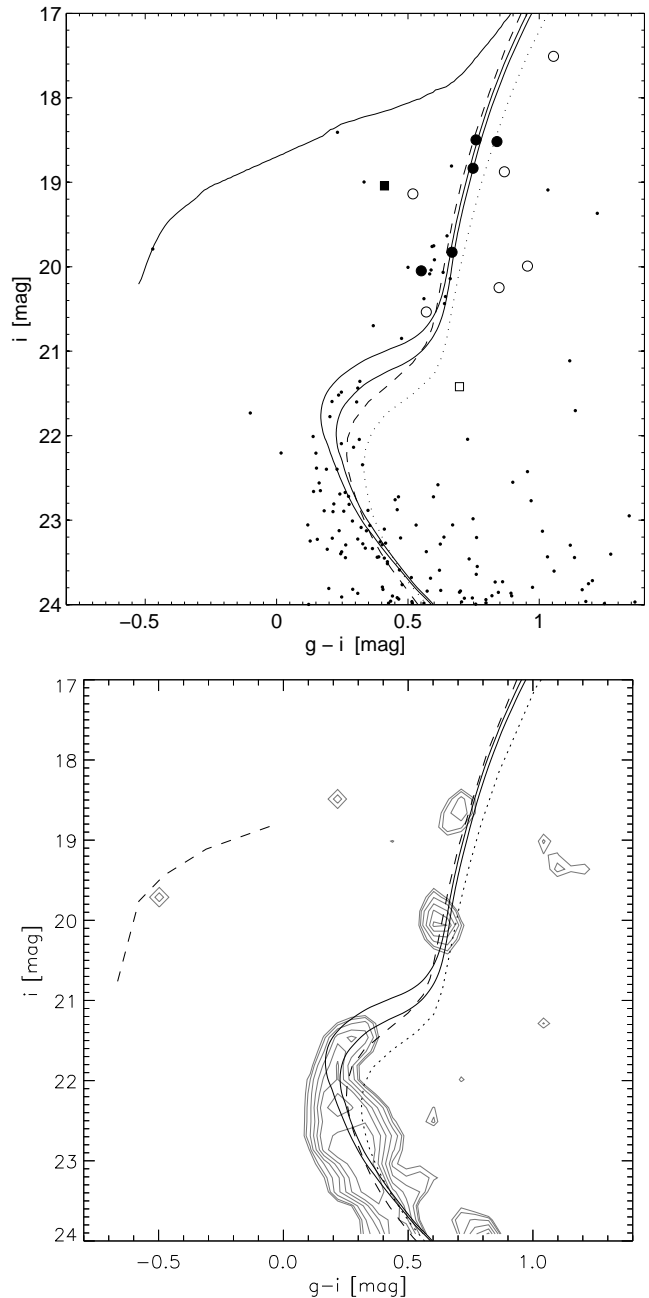


FIG. 6.— CMD for stars within $3'$ of the center of Boo II, with our spectroscopic target stars indicated (top panel). We distinguish possible Boo II members (solid circles) from probable non-members (open circles). The bottom panel shows a foreground-subtracted Hess diagram of the same region. In both panels, the solid black lines show 10 and 12 Gyr Dartmouth isochrones with $[\text{Fe}/\text{H}]=-1.8$ dex (Dotter et al. 2008), shifted to a distance modulus of 18.3. Also indicated are the fiducials of M92 (dashed; $[\text{Fe}/\text{H}]=-2.4$ dex) and M13 (dotted; $[\text{Fe}/\text{H}]=-1.5$ dex) from Clem et al. (2008). (Note that the HB bottom panel is the fiducial line for M92, as opposed to the theoretical isochrones’ HB shown in the top panel). Our five possible Boo II members follow the RGB of the isochrone. The velocity outlier with $v_{\text{HC}} = -166 \text{ km s}^{-1}$ (solid square) falls below the horizontal branches of all the isochrones, and is therefore likely to be a foreground dwarf. For completeness, the star with an ambiguous cross-correlation peak is shown as an open square.

km s^{-1} falls ~ 1 mag below the HB of any of the isochrone models, which indicates that it is most likely a foreground star. All of the other five suspected Boo II member candidates in the radial velocity peak at $\sim -120 \text{ km s}^{-1}$ directly follow the RGB of the “best-fit” isochrone, from which we conclude that these stars in fact constitute a detection of Boo II red giant members.

3.4. Metallicities

We estimated stellar metallicities from the well-established CaT lines indicator (e.g., Koch et al. 2006). To this end, we measured the equivalent widths (EWs) of each line by fitting a Gaussian plus Lorentz profile (Cole et al. 2004) and integrating the respective function over the line band passes defined by Armandroff & Zinn (1988). Given the low S/N ratio of our data, we also chose to integrate the lines numerically over the standard band passes as a sanity check; both methods yield consistent values with a mean deviation of 0.01 dex (r.m.s. scatter of 0.18 dex). In practice, we combine the CaT EWs into a line strength $\Sigma W = 0.5 \text{EW}(8498) + \text{EW}(8542) + 0.6 \text{EW}(8662)$, where we use the calibrations of Rutledge et al. (1997a; 1997b) onto the Galactic GC scale of Carretta & Gratton (1997) to obtain the final metallicities that are stated in Table 1. That is, $[\text{Fe}/\text{H}] = -2.66 + 0.42 [\Sigma W + 0.64 (V - V_{\text{HB}})]$. Here, V is our INT-based V-band magnitude and V_{HB} denotes the magnitude of the HB. Given the sparsity of the HB in the observed CMD (see Figure 1), this value could not be directly determined from our observations, nor is it well constrained from the previous photometric studies (Walsh et al. 2007a,b). Thus we relied on the locus of the *theoretical HB* from the best-fit isochrone (Sect. 3.2). One should note that this isochrone fit relied, in turn, on an adopted metallicity that is *a priori* unknown. As it transpires, however, the best-fit value of $V_{\text{HB}} = 18.5 \pm 0.2$ mag is fairly insensitive to a broader range in metallicity and the quoted systematic uncertainty reflects this initial ignorance and also accounts for unknown age and metallicity variations within the galaxy’s stellar populations (Cole et al. 2004; Koch et al. 2006). Overall, the mean *random* error on our metallicities given in Table 1 is 0.16 dex. Fig. 7 shows the derived metallicities as a function of radial velocity.

Those stars in the velocity clump at $\sim -120 \text{ km s}^{-1}$ also show very similar metallicities at around -1.8 dex. On the other hand, the presumed Galactic foreground contamination at higher velocities is well separated from Boo II in that these stars show systematically higher “metallicities” with a broad scatter. Since the distances to these stars are unknown and the CaT is not a well-calibrated metallicity indicator for such dwarf stars, application of the CaT calibrations to the foreground component will naturally result in an arbitrary metallicity assignment. The object that has an ambiguous velocity measurement deviates by $\sim 5\sigma$ from the mean metallicity, which is consistent with its being a foreground star. As an independent test, we also measured the EW of the gravity sensitive Na doublet lines at 8183, 8195 Å. These are generally weak in red giants, but show up strongly in dwarf spectra (e.g., Schiavon et al. 1997) and are thus a powerful dwarf/giant discriminator (e.g., Koch et al. 2008). While we do not attempt to per-

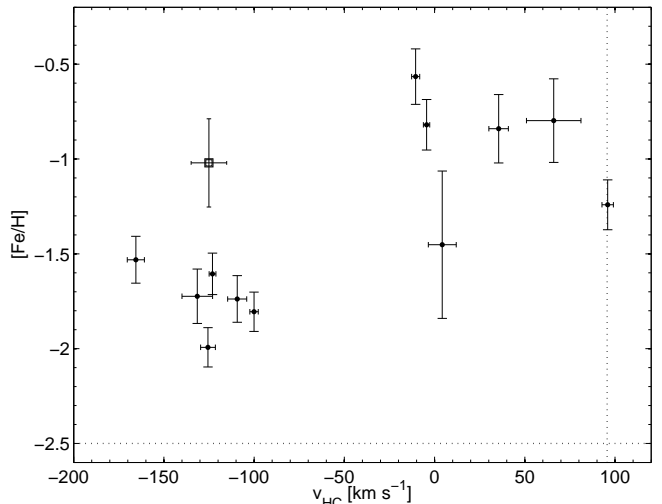


FIG. 7.— Spectroscopic metallicity versus radial velocity for all stars with good velocity measurements. The apparent non-member with an ambiguous velocity estimate is indicated with an open square. The dashed lines delineate the mean values of velocity and $[\text{Fe}/\text{H}]$ for Boötes I (Muñoz et al. 2006).

form a membership separation from this indicator, we note that those stars with velocities below -50 km s^{-1} have systematically lower Na widths (with a mean and 1σ scatter of $0.28 \pm 0.36 \text{ \AA}$) than those at higher velocities ($0.76 \pm 0.34 \text{ \AA}$). With a width of $1.94 \pm 0.51 \text{ \AA}$, the object with the spurious velocity has a Na width which is 2.7σ larger than those of the potential Boo II giant members, thus strengthening the argument that it is a foreground dwarf.

3.5. The characteristics of Boötes II

The mean radial velocity and dispersion of *all* stars below -50 km s^{-1} are -125 and 19 km s^{-1} , respectively. This is an unrealistically high dispersion and we note that the object with the most negative velocity in our sample, at -166 km s^{-1} , lies below the mean velocity value by at least 2σ , independent of its inclusion or exclusion from the Boo II member sample. Considering its location in the CMD (Fig. 6), we will treat this star as a likely non-member for the remainder of this work. The star with the dubious velocity value does not alter the mean and dispersion by more than 0.8 km s^{-1} , but its CMD position and its metallicity argue against an association with Boo II and we will not include it in the further discussions.

This leaves five red giant member candidates with a mean systemic velocity of $(-117.0 \pm 5.2) \text{ km s}^{-1}$ and a velocity dispersion of $(10.5 \pm 7.4) \text{ km s}^{-1}$, as determined using a maximum likelihood estimator. If we compare this value to the systemic velocity for Boötes I of $+95.6 \pm 3.4 \text{ km s}^{-1}$ (Muñoz et al. 2006), $99.0 \pm 2.1 \text{ km s}^{-1}$ (Martin et al. 2007), respectively, as indicated by the arrow in Fig. 5, any physical connection between these two systems is firmly ruled out. Taken at face value, the dispersion is comparable to the values observed in almost all of the luminous Local Group dSphs (e.g., Walker et al. 2007; Gilmore et al. 2007), while the dispersions of the ultrafaint dSphs (to which Boo II clearly belongs) are typically $5\text{--}7 \text{ km s}^{-1}$ and thus systematically lower (Simon & Geha 2007). The determination of more ve-

locities of likely Boo II members is necessary to constrain the internal kinematic properties of this system.

For our five member stars we find a mean metallicity of (-1.79 ± 0.05) dex on the scale of Carretta & Gratton (1997) with a 1σ -dispersion of 0.14 dex, and 0.08 dex after correction for measurement uncertainties, respectively. This spectroscopic mean is higher than the photometric estimate by Walsh et al. (2007b). By comparison with a fiducial of the old (12 Gyr), metal poor (-2.4 dex), α -enhanced GC M92, these authors argue that there is an “apparent match” between the cluster and Boo II’s populations, although a somewhat higher metallicity is not ruled out by the data, given the sparse RGB. The most metal poor star in our sample lies at -2 dex and an overlap with a more metal poor component is thus not excluded.

4. ON THE NATURE OF BOÖTES II

The immediate comparison of our derived radial velocities and metallicities of Boo II with those of the Boötes I dSph (dashed lines in Fig. 6; Muñoz et al. 2006; Martin et al. 2007) rules out any physical connection between these systems. While a difference in mean metallicity of ~ 0.7 dex is not critical, it is difficult to envision two physically associated dwarf galaxies with a relative velocity difference of ~ 200 km s $^{-1}$.

Although it is tempting to identify Boo II with the classical dSphs (i.e., an old, metal poor system associated with a single dark matter halo) based on its stellar population, this interpretation is complicated by its astrophysical environment, which we now explore.

4.1. Sagittarius

At $(\alpha, \delta) = (209.5^\circ, 12.9^\circ)$ Boo II lies in projection at the edge of the northern, leading arm of the Sagittarius (Sgr) Stream (Ibata et al. 1997, 2001; Majewski et al. 2003; Belokurov 2006b). Both the stellar populations (e.g., Newberg et al. 2002; Majewski et al. 2003; Belokurov et al. 2006b) of the latter feature, its observed kinematics (Majewski et al. 2004) and subsequent simulations (Law et al. 2005; Fellhauer et al. 2006) suggest that at least one wrap of the stream’s leading arm passes at a heliocentric distance of ~ 40 kpc and that its stars exhibit radial velocities around -100 km s $^{-1}$, similar to that found for Boo II. This leads to the natural suggestion that Boo II may constitute the remnant of a dSph or star cluster, or a density enhancement (or a tidal dwarf) that was associated with the Sgr dSph or the progenitor thereof.

We also note a small excess of stars in the offset control field that coincide with location of the main sequence of Boo II. A Hess diagram reveals that such a feature is fully compatible with noise. If real, that feature would be closer than expected for the leading branch of Sgr and might constitute the trailing arm that wrapped around the entire Galaxy. There is also photometric evidence for a narrow stream that passes the Boo region of the sky and emerges from Sgr (e.g., Fig. 1 of Belokurov et al. 2006b).

In Fig. 8, we overplot the location of Boo II in Galactic coordinates (adopting the distance estimate from the present work) and our measured radial velocities on the simulations of Fellhauer et al. (2006), which are color-coded by the time when the particles were removed from

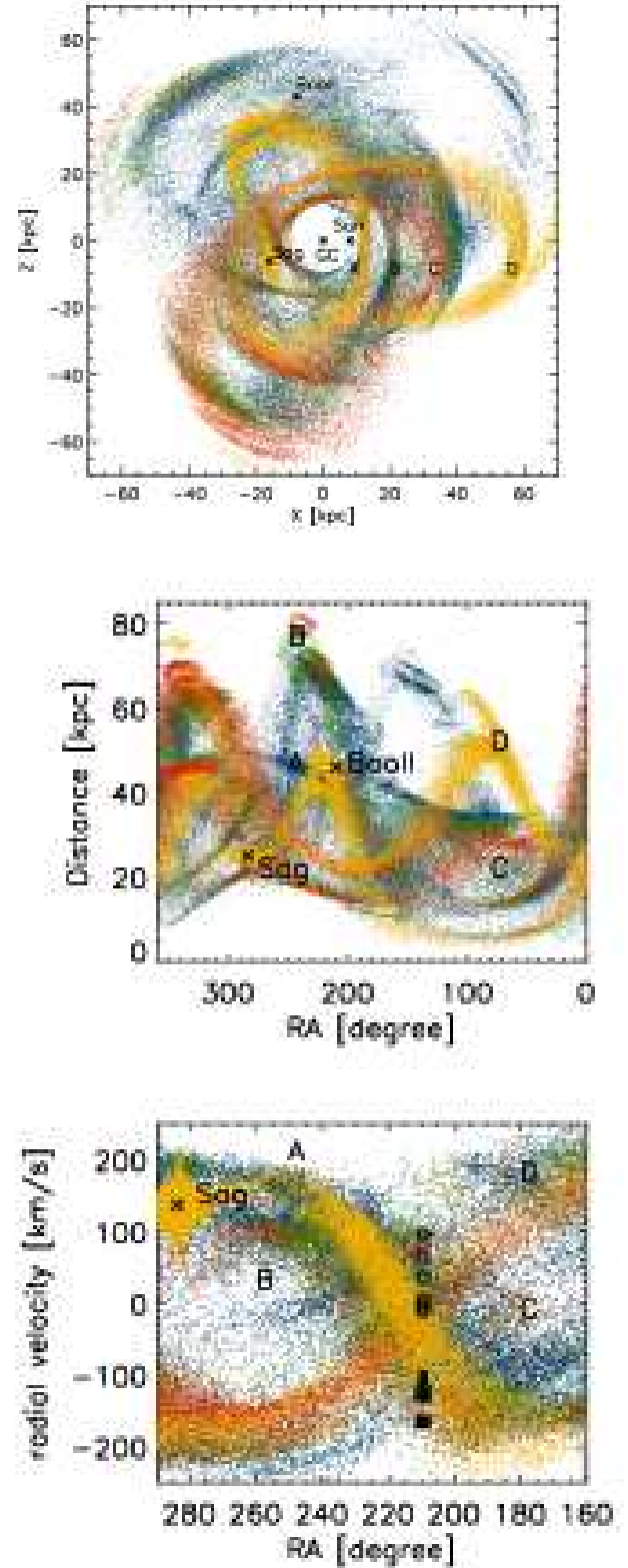


FIG. 8.— Top and middle panels: Location of Boo II (black points) on the simulations of Fellhauer et al. (2006) of the Sgr Stream. This assumes a distance to Boo II of 46 kpc as estimated in this work. The simulation particles are color coded according to the time they were lost from Sgr (gold: <4 Gyr ago; red: 4–5.7 Gyr; green: 5.7–7.4 Gyr; blue: >7.4 Gyr ago). The bottom panel indicates all our good velocity points on the same simulations, using the same symbols as in Fig. 6. An association of Boo II with Sgr is thus feasible.

Sgr. As this comparison illustrates, both the distance and the radial velocity range of Boo II are *consistent with an association with the Sgr Stream*. In particular, its location (top panel of Fig. 8) suggests a relation with branch “A”, that is the “young leading arm” according to Belokurov et al. (2006b) and Fellhauer et al. (2006). The simplistic illustration in the middle and bottom panels of Fig. 8 appears to favor a stripping of this feature 4–5.7 Gyr ago (red points) or perhaps earlier than 7.4 Gyr ago (blue points in the simulations). Given the limited extent of our data we refrain from overinterpreting any dynamical history of Boo II. We note in passing that the foreground stars at higher velocities also fall on top of the stream points.

Note that, at an $[\text{Fe}/\text{H}]$ of -1.79 dex, Boo II is more metal-poor than the dominant stellar population in the core of the Sgr dwarf, which has a mean metallicity of ~ -0.4 dex (Smecker-Hane & McWilliam 2002; Bonifacio et al. 2004; Monaco et al. 2005; Sbordone et al. 2007) but exhibits a broad range in metallicity from ~ -1.6 dex to Solar, and more metal poor than the predominant field population of the stream (e.g., Monaco et al. 2007). On the other hand, based on the significant variations of the metallicity distributions along the leading arm, Chou et al. (2007) argue that there must have been a strong metallicity gradient present in the Sgr progenitor (see also Bellazzini et al. 2006). Moreover, Vivas et al. (2005) find that a sample of RR Lyrae stars in the leading arm is clearly metal poor, at a mean $[\text{Fe}/\text{H}]$ of -1.76 dex. One possible explanation is thus that Boo II is a mere overdensity in the Sgr stream, resembling its known old and metal poor subpopulation.

Likewise, it is conceivable that Boo II is a coherent system that has been tidally stripped from Sgr. There is currently a multitude of GCs assigned to Sgr and its stream system (Ibata et al. 1997; van den Bergh 1998; Palma et al. 2002; Bellazzini et al. 2003). Those GCs show a broad range in $[\text{Fe}/\text{H}]$ from the mean of the Sgr dSph (-0.5 dex; e.g., Ibata et al. 1997; Brown et al. 1999; Bellazzini et al. 2002; Cohen 2004; Sbordone et al. 2005) down to -2 dex (Da Costa & Armandroff 1995) and Boo II falls in this range. With a half-light radius of (56 ± 12) pc, Boo II is definitely too extended to be a classical GC and it is also larger than the confirmed Sgr clusters (with $r_h \lesssim 13$ pc). In the radius-vs.- M_V plot (e.g., Figure 1 of Gilmore et al. 2007), Boo II lies in the gap between the Local Group dSphs and the Galactic GCs. Although this system is significantly fainter than the GCs, it is a factor of 5–10 larger in r_h and thus comparable in size to the ultrafaint Com Ber, Segue 1 (Belokurov et al. 2007) and Willman 1 (Willman et al. 2005b) objects. Coupled with the large velocity dispersion found in this work, this argues against Boo II being a GC, but rather indicates that it is in fact an ultrafaint, compact (relative to the more luminous dwarfs) dSph-like object that may have been stripped from Sgr.

5. DISCUSSION

At the time of its discovery, the Boötes I dSph was the faintest, most metal poor and most dark matter dominated dSph known (Belokurov et al. 2006; Muñoz et al. 2006; Martin et al. 2007). Despite its high dark matter content it is apparently elongated. Fellhauer et al. (2008) argue that this does not arise due to tidal interactions,

but is rather due to flattening of the progenitor inside an extended dark matter halo. Adopting a distance to Boötes I of (66 ± 3) kpc (Dall’Ora et al. 2006) and our derived value of 46 kpc for Boo II, the implied separation between both these galaxies is (21 ± 9) kpc and thus comparable to the present-day LMC–SMC separation (e.g., Gardiner & Noguchi 1996). In contrast to Boötes I with its high positive velocity of $\sim 100 \text{ km s}^{-1}$ (Muñoz et al. 2006; Martin et al. 2007), the fainter Boo II dSph exhibits a much lower systemic velocity of -117 km s^{-1} . A relative velocity difference of $\sim 200 \text{ km s}^{-1}$ is inconsistent with a gravitational association between Boötes I and II, and is inconsistent with them being on the same orbit through the Galaxy.

Another important difference between these projected neighbors lies in their mean metallicities. With a mean $[\text{Fe}/\text{H}]$ of ~ -2.5 , Boötes I represents the most metal poor dSph known to date (Muñoz et al. 2006)⁷. The fainter Boo II is found to have a higher mean value of -1.79 dex, which is compatible with a number of the more luminous dSphs (e.g., Grebel et al. 2003).

Dwarf galaxies follow well-known metallicity-luminosity and mass-metallicity relations (Dekel & Woo 2003; Grebel et al. 2003; Martin et al. 2007), where the more massive galaxies exhibit higher metallicity. This is explicable in terms of the deeper potential wells of the massive systems, allowing for gas to be retained for a longer time, leading to more efficient enrichment. Martin et al. (2008) estimate a stellar mass in the range of $3.7\text{--}7.2 \times 10^4 M_\odot$ for Boo II, depending on the adopted Initial Mass Function. With the spectroscopic estimate from this work, Boo II is significantly more metal rich (by 1 dex) than the value implied by an extrapolation of the fundamental scaling relation of the more luminous low-surface brightness galaxies and Local Group dwarfs (Dekel & Woo 2003). Adding Boo II to the presently available spectroscopic data of the ultrafaint dSphs (e.g., Fig. 11 in Simon & Geha 2007) indicates that a linear relation between luminosity and metallicity breaks down for systems fainter than $M_V \gtrsim -5$ mag. In fact, it appears that such a relation shows an upturn towards higher metallicities for the faintest systems.

The interpretation of the lowest-luminosity dwarfs in terms of a tidally stripped remnant (e.g. UMa II, Com Ber; Simon & Geha 2007; Martin et al. 2008) or association with the Sgr dwarf (Boo II; this work) then begs the question of whether these objects constitute a satellite population distinct from the higher-luminosity dSphs. It is interesting that both Boo II and Coma Berenices, the two galaxies which have half-light radii smaller than the apparent ~ 100 pc limit identified by Gilmore et al. (2007) and are close to the Galactic centre, also have mean metallicities which are high relative to the trend defined by all other dSph galaxies. This is consistent with these objects being the surviving remnants of parent dSphs which were originally several magnitudes brighter, and which followed the luminosity-metallicity trend, and possibly also the minimum-size relation.

⁷ Martin et al. (2007) find a slightly more metal rich mean of $[\text{Fe}/\text{H}] = -2.1$ dex, which may be related to the adopted calibrations of the metallicity scale and extrapolations of these calibrations towards the metal poor end.

The nature of Boo II is far from clear. Given the detection of distinct, though sparse, CMD features and the kinematic and chemical evidence derived in this work, we are left with three possible interpretations of our spectroscopic detection at -117 km s^{-1} :

1. The overdensity is Boo II itself and it is an old and moderately metal poor dSph. The distinct MSTO in the CMD (Fig. 1; Walsh et al. 2007a,b) argues in favor of this interpretation. The anomalously small half-light radius, which we estimate as $4.0^{+0.7}_{-0.3}$ (56^{+8}_{-6} pc), and anomalously high mean chemical abundance, together with its Galactic environment, are consistent with this being the surviving remnant of a larger and more luminous dSph. Our measured velocity dispersion ($10.5 \pm 7.4 \text{ km s}^{-1}$) is too uncertain to allow us to derive a reliable mass-to-light ratio, or even to test the hypothesis that Boo II is close to internal dynamical equilibrium.
2. Comparison with simulations of the Sagittarius stream suggests that Boo II may be a dissolved cluster or a disrupted dSph formerly associated with Sagittarius. The metallicities of our Boo II stars are consistent with those found in a broad range of Sgr populations and GCs, and is also consistent with the Stream's old and metal poor field population (Vivas et al. 2005). We note that the large radius of Boo II is consistent with a disrupting star cluster for only a very brief time, so that it is

unlikely that such a rare event would be observed. Similarly, a star cluster in late disruption has an internal velocity dispersion of almost zero km s^{-1} (cf. Küpper et al. 2008). Thus, it is unlikely that Boo II is an unbound, purely stellar system observed at a special time.

3. Last, and least comforting, we may have simply not targeted any of the real Boo II stars. Given the clumping in velocity, CMD, and metallicity this appears unlikely. Moreover, this option would imply that the galaxy's real RGB may in fact be even sparser than the apparent feature in the CMD, yielding an even lower luminosity and mass.

AK would like to thank the University of Leicester for hosting a generous stay, during which this work was carried out. MIW acknowledges support from a Royal Society University Research Fellowship. Based on observations obtained at the Gemini Observatory, which is operated by the Association of Universities for Research in Astronomy, Inc., under a cooperative agreement with the NSF on behalf of the Gemini partnership: the National Science Foundation (United States), the Science and Technology Facilities Council (United Kingdom), the National Research Council (Canada), CONICYT (Chile), the Australian Research Council (Australia), CNPq (Brazil) and SECYT (Argentina)

REFERENCES

- Armandroff, T. E., & Zinn, R. 1988, *AJ*, 96, 92
 Bellazzini, M., Ferraro, F. R., & Ibata, R. 2003, *AJ*, 125, 188
 Bellazzini, M., Newberg, H. J., Correnti, M., Ferraro, F. R., & Monaco, L. 2006, *A&A*, 457, L21
 Belokurov, V., et al. 2006a, *ApJ*, 647, L111
 Belokurov, V., et al. 2006b, *ApJ*, 642, L137
 Belokurov, V., et al. 2007, *ApJ*, 654, 897
 Bonifacio, P., Sbordone, L., Marconi, G., Pasquini, L., & Hill, V. 2004, *A&A*, 414, 503
 Bovill, M. S., & Ricotti, M. 2008, *ArXiv e-prints*, 806, arXiv:0806.2340
 Brown, J. A., Wallerstein, G., & Gonzalez, G. 1999, *AJ*, 118, 1245
 Carretta, E., & Gratton, R. 1997, *A&AS*, 121, 95
 Chou, M.-Y., et al. 2007, *ApJ*, 670, 346
 Clem, J. L., Vanden Berg, D. A., & Stetson, P. B. 2008, *AJ*, 135, 682
 Cohen, J. G. 2004, *AJ*, 127, 1545
 Cole, A. A., Smecker-Hane, T. A., Tolstoy, E., Bosler, T. L., & Gallagher, J. S. 2004, *MNRAS*, 347, 367
 Dall'Ora, M., et al. 2006, *ApJ*, 653, L109
 Da Costa, G. S., & Armandroff, T. E. 1995, *AJ*, 109, 2533
 Dekel, A., & Woo, J. 2003, *MNRAS*, 344, 1131
 Dotter, A., Chaboyer, B., Jevremovic, D., Kostov, V., Baron, E., & Ferguson, J. W. 2008, *ApJS*, 178, 89
 Fellhauer, M., et al. 2006, *ApJ*, 651, 167
 Fellhauer, M., Wilkinson, M. I., Evans, N. W., Belokurov, V., Irwin, M. J., Gilmore, G., Zucker, D. B., & Kleyna, J. T. 2008, *MNRAS*, 385, 1095
 Font, A. S., Johnston, K. V., Bullock, J. S., & Robertson, B. E. 2006, *ApJ*, 638, 585
 Gardiner, L. T., & Noguchi, M. 1996, *MNRAS*, 278, 191
 Gilmore, G., Wilkinson, M. I., Wyse, R. F. G., Kleyna, J. T., Koch, A., Evans, N. W., & Grebel, E. K. 2007, *ApJ*, 663, 948
 Grebel, E. K., Gallagher, J. S., III, & Harbeck, D. 2003, *AJ*, 125, 1926
 Ibata, R. A., Wyse, R. F. G., Gilmore, G., Irwin, M. J., & Suntzeff, N. B. 1997, *AJ*, 113, 634
 Ibata, R., Irwin, M., Lewis, G. F., & Stolte, A. 2001, *ApJ*, 547, L133
 Irwin, M., & Lewis, J. 2001, *New Astronomy Review*, 45, 105
 Kleyna, J. T., Wilkinson, M. I., Evans, N. W., & Gilmore, G. 2004, *MNRAS*, 354, L66
 Koch, A., Grebel, E. K., Wyse, R. F. G., Kleyna, J. T., Wilkinson, M. I., Harbeck, D. R., Gilmore, G. F., & Evans, N. W. 2006, *AJ*, 131, 895
 Koch, A., et al. 2008, *ApJ*, in press (astro-ph/0711.4588)
 Küpper, A. H. W., MacLeod, A., & Heggie, D. C. 2008, *MNRAS*, 387, 1248
 Landolt, A. U. 1992, *AJ*, 104, 340
 Law, D. R., Johnston, K. V., & Majewski, S. R. 2005, *ApJ*, 619, 807
 Majewski, S. R., Skrutskie, M. F., Weinberg, M. D., & Ostheimer, J. C. 2003, *ApJ*, 599, 1082
 Majewski, S. R., et al. 2004, *AJ*, 128, 245
 Martin, N. F., Ibata, R. A., Chapman, S. C., Irwin, M., & Lewis, G. F. 2007, *MNRAS*, 380, 281
 Martin, N. F., de Jong, J. T. A., & Rix, H.-W. 2008, *MNRAS*, in press (astro-ph/0805.2945)
 Mateo, M. L. 1998, *ARA&A*, 36, 435
 Monaco, L., Bellazzini, M., Bonifacio, P., Ferraro, F. R., Marconi, G., Pancino, E., Sbordone, L., & Zaggia, S. 2005, *A&A*, 441, 141
 Monaco, L., Bellazzini, M., Bonifacio, P., Buzzoni, A., Ferraro, F. R., Marconi, G., Sbordone, L., & Zaggia, S. 2007, *A&A*, 464, 201
 Moore, B., Ghigna, S., Governato, F., Lake, G., Quinn, T., Stadel, J., & Tozzi, P. 1999, *ApJ*, 524, L19
 Muñoz, R. R., Carlin, J. L., Frinchaboy, P. M., Nidever, D. L., Majewski, S. R., & Patterson, R. J. 2006, *ApJ*, 650, L51
 Newberg, H. J., et al. 2002, *ApJ*, 569, 245
 Palma, C., Majewski, S. R., & Johnston, K. V. 2002, *ApJ*, 564, 736
 Robertson, B., Bullock, J. S., Font, A. S., Johnston, K. V., & Hernquist, L. 2005, *ApJ*, 632, 872

- Robin, A. C., Reyl e, C., Derri ere, S., & Picaud, S. 2003, *A&A*, 409, 523
- Rutledge, G.A., Hesser, J.E., Stetson, P.B., Mateo, M., Simard, L., Bolte, M., Friel, E.D., & Copin, Y. 1997a, *PASP*, 109, 883
- Rutledge, G.A., Hesser, J.E., Stetson, P.B. 1997b, *PASP*, 109, 907
- Sbordone, L., Bonifacio, P., Marconi, G., Buonanno, R., & Zaggia, S. 2005, *A&A*, 437, 905
- Sbordone, L., Bonifacio, P., Buonanno, R., Marconi, G., Monaco, L., & Zaggia, S. 2007, *A&A*, 465, 815
- Schiavon, R. P., Barbuy, B., Rossi, S. C. F., & Milone, A. 1997, *ApJ*, 479, 902
- Schlegel, D. J., Finkbeiner, D. P., & Davis, M. 1998, *ApJ*, 500, 525
- Siegel, M. H. 2006, *ApJ*, 649, L83
- Smecker-Hane, T. A., & McWilliam, A. 2002, *ArXiv Astrophysics e-prints*, arXiv:astro-ph/0205411
- Strigari, L. E., Bullock, J. S., Kaplinghat, M., Diemand, J., Kuhlen, M., & Madau, P. 2007, *ApJ*, 669, 676
- Unavane, M., Wyse, R. F. G., & Gilmore, G. 1996, *MNRAS*, 278, 727
- van den Bergh, S. 1998, *ApJ*, 505, L127
- Venn, K. A., Irwin, M., Shetrone, M. D., Tout, C. A., Hill, V., & Tolstoy, E. 2004, *AJ*, 128, 1177
- Vivas, A. K., Zinn, R., & Gallart, C. 2005, *AJ*, 129, 189
- Walker, M. G., Mateo, M., Olszewski, E. W., Gnedin, O. Y., Wang, X., Sen, B., & Woodroffe, M. 2007, *ApJ*, 667, L53
- Walsh, S. M., Jerjen, H., & Willman, B. 2007a, *ApJ*, 662, L83
- Walsh, S. M., Willman, B., Sand, D., Harris, J., Seth, A., Zaritsky, D., & Jerjen, H. 2007b, *ApJ*, in press (astro-ph/0712.3054)
- Willman, B., et al. 2005a, *ApJ*, 626, L85
- Willman, B., et al. 2005b, *AJ*, 129, 2692
- Zucker, S. 2003, *MNRAS*, 342, 1291
- Zucker, D. B., et al. 2006, *ApJ*, 643, L103